

Nuclear Characteristics and Safety Analysis of Neutron Absorbers in Core-Loaded Irradiation Rig

Hae Sun Jeong*, Sung Jae Park, Seong Woo Yang, Kee Nam Choo, Yoon Taeg Shin, Chul Yong Lee, Dong-Joo Kim,
and Jae-Yong Kim

Korea Atomic Energy Research Institute, 111, Daedeok-daero 989beon-gil, Yuseong-gu, Daejeon, Korea

*Corresponding author: haesunin@kaeri.re.kr

1. Introduction

Recently, the Korea Atomic Energy Research Institute has been developing high-performance neutron absorber materials to improve the vulnerability of existing control rods as part of the safety-reinforcement technology for APR reactor core [1].

The neutron absorber B_4C in control rods can cause an eutectic reaction with Inconel-625 or STS mainly used as the cladding material, when the temperature rises. When B_4C is exposed to air due to damage to the cladding, oxidation starts at about 600-700°C and it volatilizes at about 1500°C, and a large amount of hydrogen may be generated during this process. In addition, in the event of a control rod accident, the possibility of re-criticality due to fail of neutron control should be taken account not to be insignificant. Therefore, a new design of neutron absorbers with high-performance is a necessary part to reinforce the safety of APR reactor core.

Currently, the candidate groups for a development of neutron absorber materials are composed of combinations based on various types of oxides such as Eu_2O_3 , Dy_2O_3 , ZrO_2 , TiO_2 , and HfO_2 . Accordingly, a series of irradiation tests on the neutron absorbers designed with various compositions will be performed using the HANARO research reactor.

This study is performed to verify the nuclear characteristics and safety of neutron absorber materials for control rods through MCNP6 [2] Monte Carlo analysis prior to conducting the irradiation tests. The analysis results include the reactivity changes in irradiation tests, the neutron flux distribution, and the neutron and gamma-ray heat generation along with the position of the control rods. However, only a part of results (OR3, CAR 350 mm) was included in this paper, and the whole results are included in detail in the recently published report [3].

2. Computational Core Model for Irradiation Test

The HANARO multipurpose research reactor is an open-water tank type and is cooled by the upward forced convection with light water. Figure 1 shows the major devices including some kinds of irradiation holes installed in and around the reactor core. The inner core contains 23 hexagonal flow tubes, including CT, IRs, and CARs and SORs of cylindrical flow tubes. To perform an irradiation test in the most appropriate

environments possible, it is important to select a suitable irradiation hole considering test safety aspects on reactivity and nuclear characteristics such as neutron flux distributions or heat generation.

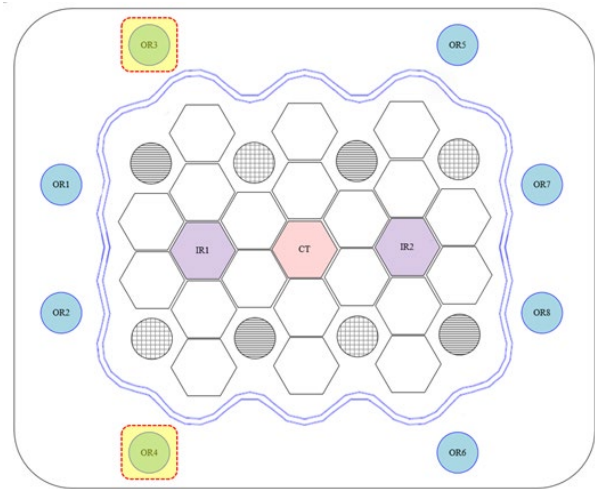


Fig. 1. Radial arrangement model of major devices in and around HANARO reactor core

In this study, OR3 and OR4 irradiation holes were selected to ensure sufficient neutron flux suitable to evaluate the nuclear characteristics of the neutron absorber for control rods. The core conditions for the computational analysis of the irradiation test are as follows.

- Reactor power: 30 MW
- Core status: equilibrium core
- Control rod positions: 350 mm, 450 mm, and 545 mm above the lower part of the fuel
- Irradiation holes: OR3 and OR4
- Internal conditions of the irradiation hole:
 - w/ neutron absorbers
 - w/o neutron absorbers (i.e., filled with water excluding internal structure)

The neutron absorbers currently under development are composed of a combination based on oxides such as Eu_2O_3 , Dy_2O_3 , ZrO_2 , TiO_2 , and HfO_2 , which could replace the neutron absorber for the existing control rod. Table 1 summarizes the main physical properties of selected materials at the upper and lower parts of the irradiation rig. The irradiation test analysis was performed based on these 16 kinds of compositions.

The atomic mass and atomic density shown in the table are the amounts for the mixture of each neutron absorber material.

Table 1. Properties of neutron absorber materials

	Neutron Absorber (ID)	Density [g/cc]	Atomic Mass [g/mol]	Atomic Density [#/cm ³]
U P P E R	U1D	8.75	534.91	9.85E+21
	U2B	1.76	55.24	1.92E+22
	U3E	7.2	362.45	1.20E+22
	U4D	7.4	372.98	1.19E+22
	U5D	7.5	780.41	5.79E+21
	U6D	6.5	692.36	5.65E+21
	U7D	7.6	352.15	1.30E+22
	U8D	7.6	337.67	1.35E+22
L O W E R	L1E	6.23	446.97	8.39E+21
	L2E	6.85	490.33	8.41E+21
	L3E	8.08	562.39	8.65E+21
	L4B	1.76	55.24	1.92E+22
	L5D	7.65	175.83	2.62E+22
	L6D	7.65	180.16	2.56E+22
	L7D	7.9	188.89	2.52E+22
	L8D	7.4	496.19	8.98E+21

On the other hand, in order to use more appropriate nuclear data in the analysis process, it is necessary to calculate the atomic density for each isotope. The atomic density (N) of the mixture (m) consisting of isotopes X and Y is as follows,

$$N_m = \frac{\rho_m N_A}{M_m} \quad (1)$$

Based on the atomic density of the mixture, therefore, the atomic density for each isotope according to the composition ratio was calculated. The atomic densities of all finally calculated isotopes are presented in the KAERI technical report [3].

Figure 2 (a) shows the arrangement of the OR3 irradiation hole around the reactor core, and (b) shows the capsule-loaded shape modeled by MCNP6. One zig is built into the upper and lower parts of the irradiation hole individually, and one single zig contains eight circular irradiation capsules. The material numbers in the irradiation capsule were determined in the clockwise order for both the upper and lower zigs. A total of 16 capsules are loaded with different neutron absorbers in order, and the inside of the capsules is filled with He gas. The nuclear analysis of the OR3 and OR4 holes was performed independently.

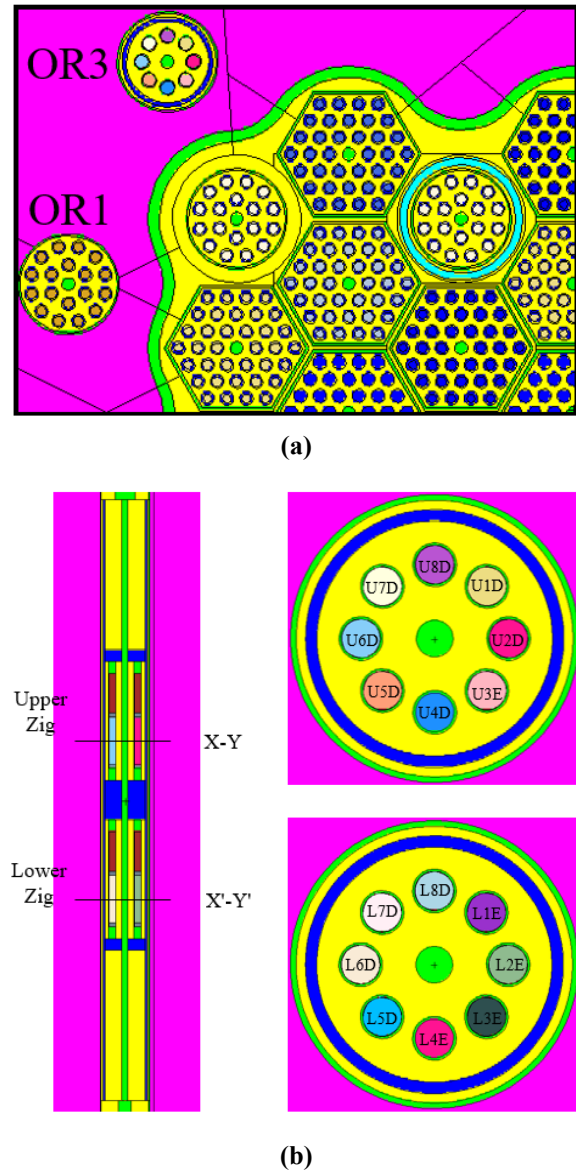


Fig. 2. (a) Arrangement of OR3 irradiation hole around the reactor core, (b) Axial model of irradiation rig and radial loading pattern of neutron absorbers in the upper and lower zigs (MCNP6)

3. Results for Nuclear Characteristics and Safety

3.1. Reactivity Change

During the reactor irradiation test, the reactivity may change rapidly due to abnormal withdrawal of the irradiation material in the irradiation hole.

Therefore, the reactivity was evaluated to confirm the safety of the irradiation test using the OR irradiation holes based on the criterion for safety evaluation [3]. For the calculations of the BOC, the MOC, and the EOC of the equilibrium core, the control rods were assumed to be positioned at 350 mm, 450 mm, and 545 mm, respectively.

Table 2. Reactivity changes with and without neutron absorbers by control rod position

Irrad. Hole	CAR Position [mm]	w/ Neutron Absorbers		w/o Neutron Absorbers		Reactivity $\Delta \rho$ [mk]
		k_{eff}	S.D.	k_{eff}	S.D.	
OR3	350	1.00790	± 0.00007	1.00864	± 0.00007	0.728
	450	1.03378	± 0.00007	1.03472	± 0.00007	0.879
	545	1.05401	± 0.00007	1.05488	± 0.00007	0.782
OR4	350	1.00816	± 0.00007	1.00887	± 0.00007	0.698
	450	1.03404	± 0.00007	1.03476	± 0.00007	0.673
	545	1.05399	± 0.00008	1.05500	± 0.00007	0.908

Table 2 shows that the reactivity in the core is inserted according to the loading of the neutron absorber material for each control rod position in the two irradiation holes. The calculation errors were found to be about 7 pcm for all cases. In case that the irradiation hole does not contain absorbers, the structures in other remaining irradiation holes are modeled as they are, but the target hole is assumed to be filled with water without including the structure. In addition, the keff values in the absence of absorber of OR3 and OR4 are evaluated differently, since the structures around the holes are not symmetrical. As a result, in the case of OR3, where the position of the control rod was 450 mm, the highest reactivity was inserted. The highest reactivity of OR4 was inserted in a situation where the control rod was almost withdrawn (545 mm). Nevertheless, the reactivity evaluated in both irradiation holes was less than 1 mk, which was found to be far below the limit value for the irradiation test. Therefore, it was confirmed that the irradiation tests under the aforementioned core conditions sufficiently satisfy the safety standard.

3.2. Neutron Flux Distributions

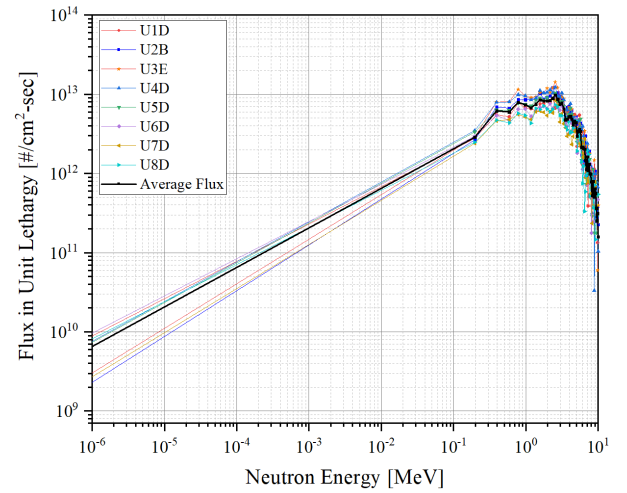
A standard tally based on a track length estimator in the Monte Carlo method was applied for the calculation of the average neutron flux ($\bar{\phi}_v$) for neutron absorbers loaded into the irradiation holes.

$$\begin{aligned} \bar{\phi}_v &= \frac{1}{V} \int dE \int dt \int dV \int d\Omega \phi(r, \Omega, E, t) \\ &= \frac{1}{V} \int dE \int dV \int dl N(r, E, t) \quad (\because dl = vdt). \end{aligned} \quad (2)$$

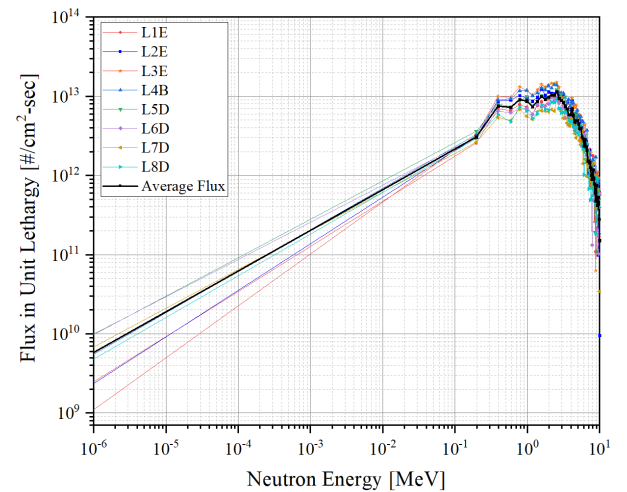
Therefore, the track length estimator of the particle trajectory is as follows.

$$\sum \frac{W}{V} \times dl \quad (\text{where, } W = \text{particle weight}). \quad (3)$$

Figures 3 show the neutron flux distributions of OR3 considering the unit lethargy (ξ) depending on the energy for the neutron absorbers calculated at the 350 mm position of CAR. In the overall results, the neutron flux in the thermal neutron region showed a very low value and gradually increased with energy, and then the neutron flux was evaluated relatively high in the $\sim 10^{-1}$ MeV to several MeV regions. This is because neutron absorbers have a high thermal absorption cross-section in common, and the neutron flux at the corresponding energy is low. This is also due to the relatively high spatial distribution of epithermal neutrons, although the OR holes are located in the outer core. Therefore, the overall tendency of the spectrum was evaluated similarly, although there was a difference in quantitative values for the neutron flux distribution by the control rod position and the material type.



(a)



(b)

Fig. 3. Neutron flux distribution per unit lethargy (ξ) in neutron absorbers charged in OR3 (a) upper part, and (b) lower part of irradiation hole

In detail, however, the each performance of the eight neutron absorbers at the upper and lower parts was somewhat different depending on the position of the irradiation hole as well as the position of the control rod. The reason is that since the reaction cross-sections of materials vary by energy, the flux distributions depending on spatial and energy affects the absorption performance.

3.3. Heat Generations from Neutrons and Gamma-rays

The heat generations from neutrons and gamma-rays were calculated through the absorption energy in each region by applying the track length tally based on Eq.(2). The average flux in each cell was the additionally considered by total macroscopic cross-section, the energy per particle collision, and the material density. This method takes into account the kinetic energy of fission products, the immediate neutrons and gamma-rays produced by fission, and photon behavior by radiation capture during neutron absorption reactions. In this study, absorption energy was evaluated by calculating a normalization factor for 29.3 MW excluding the pump power in the reactor system.

Table 3 shows the result of the heat generations from neutrons and gamma-rays for 16 neutron absorbers of OR3 at 350 mm of CAR. The statistical errors of the heat generation calculations were less than 3% for neutrons, and less than 1% for gamma-rays.

Table 3. Heat generations from neutrons and gamma-rays

	ID	From Neutrons		From Gamma-rays	
		Power [W]	Error [%]	Power [W]	Error [%]
U P P E R	U1D	2.27E-01	1.96	7.96E+01	0.73
	U2B	1.79E+02	0.82	6.43E+00	0.93
	U3E	3.30E+02	0.86	4.68E+01	0.82
	U4D	2.37E-01	1.68	7.25E+01	0.71
	U5D	2.44E-01	1.87	7.45E+01	0.71
	U6D	1.71E-01	2.07	5.79E+01	0.74
	U7D	1.49E-01	2.24	6.65E+01	0.76
	U8D	1.58E-01	2.15	6.52E+01	0.76
	Avg.	6.38E+01		5.87E+01	
L O W E R	L1E	4.30E+02	0.86	2.71E+01	0.97
	L2E	4.57E+02	0.82	3.04E+01	0.93
	L3E	4.62E+02	0.81	4.48E+01	0.88
	L4B	2.06E+02	0.76	6.78E+00	0.88
	L5D	2.57E-01	1.72	7.63E+01	0.69
	L6D	2.05E-01	1.90	7.21E+01	0.73
	L7D	1.76E-01	2.06	7.12E+01	0.73
	L8D	2.12E-01	2.01	6.09E+01	0.75
	Avg.	1.94E+02		4.87E+01	

In the case of neutron heat generation, the lower part of the OR3 irradiation rig showed relatively high level with about 400 W in L1E, L2E, and L3E regardless of the CAR position. The material L4B (B₄C), which has been mainly used as a conventional control rod material, also showed a half-level value and the next highest. In the case of OR4, the material L1E showed the highest value regardless of the CAR position. In addition, as in OR3, the material L1E, L2E, and L3E were evaluated to have relatively high values, and the material L4B also showed the next highest value. At the upper region of the irradiation rig, the material U3E was the highest heat value in OR3 and OR4, and the material U2E was the second highest.

The heat generation from gamma-rays does not have a linear relationship with those from neutrons, because various nuclear reactions occur according to the neutron absorption ratio varying with neutron energy as the chemical composition differs depending on the control material. For the lower part of the irradiation rig, the gamma-rays heat generation was evaluated in the order of L5D > L6D > L7D > L8D, showing the value of the tens of watts (W). On the other hand, the gamma-rays heat generation of L4B showed the lowest value. In the case of upper part, both OR3 and OR4 holes were rated at tens of watts except for U2B (B₄C) with several watts level.

4. Conclusions

This study describes the results of evaluating the safety and nuclear characteristics of neutron absorber materials for control rods through MCNP Monte Carlo analysis.

Accordingly, the analysis results along with the position of the control rods for two irradiation holes (OR3 and OR4) were presented including the reactivity, the flux distributions, and the heat generations from neutrons and gamma-rays. However, the detailed whole result are presented in the recently published technical report [3], and this paper includes only a part of analysis results (OR3, CAR 350 mm).

As a result of evaluating the reactivity, it was found to be less than 1 mk for both two irradiation holes. These results show that they fall far below the standard value specified in the 'HANARO operation technical guide' [4]. The irradiation test in the reactor core, therefore, would satisfy the safety criteria for reactivity insertion.

In the neutron flux evaluation according to the movement of control rods, the thermal flux showed very low and gradually increased, and the neutrons in the several MeV energy regions was evaluated to be higher than those in other regions. Quantitative differences in the neutron spectrum were found depending on a kind of irradiation hole, control rod position, or neutron absorber materials, but the overall distribution tendency along with energy was similar.

In the case of the heat generation from neutrons, L1E, L2E, and L3E showed high values at the lower part of the irradiation rig, and U3E was the highest at the upper part. The material B₄C (U2B), which has been mainly used as a neutron absorber, showed the next highest value. For the heat generation from gamma-rays, the values of L5D, L6D, L7D, and L8D were evaluated relatively high at the lower part, and U3E showed the highest at the upper part. On the other hand, the gamma heat value of B₄C showed to be the lowest at the several watts level in both upper and lower parts of the irradiation rig.

The analysis results of this study can be used as a reference for comparing nuclear characteristics with the results of irradiation tests for selecting neutron absorber materials for APR control rods, as well as proper selection of irradiation hole for future irradiation tests.

Acknowledgements

This work was supported by the Korea government (MSIT) (1711078081) and by Korea Institute of Energy Technology Evaluation and Planning (KETEP) grant funded by the Korea government (MOTIE) (No. 20217810100050).

REFERENCES

- [1] Nuclear Fuel Safety Research Division of Korea Atomic Energy Research Institute, "Report on the manufacture of irradiation swelling test specimen of neutron absorber material for control rods", KAERI-KNF-JR/APR-KETEP-2201/2022, Korea Atomic Energy Research Institute, (2022).
- [2] D. B. Pelowitz, "MCNP6TM USER'S MANUAL Version 1.0", LA-CA-13-00634, Los Alamos National Laboratory, 2013.
- [3] H. S. Jeong et al., "Analysis of Nuclear Characteristics on Neutron Absorbers for APR Control Rods", KAERI/TR-9204/2022, Korea Atomic Energy Research Institute, (2022).
- [4] J. S. Han et al., "HANARO Operation technical guide (Rev. 27)", KAERI/TR-3215/2006, Korea Atomic Energy Research Institute, (2021).